Unravelling past flash flood activity in a forested mountain catchment of the Spanish Central System

Juan A. Ballesteros-Cánovas , Clara Rodríguez-Morata , Virginia Garófano-Gómez ,
Juan M. Rubiales , Raúl Sánchez-Salguero, Markus Stoffel

Flash floods represent one of the most common natural hazards in mountain catchments, and are fre-quent in Mediterranean environments. As a result of the widespread lack of reliable data on past events, the understanding of their spatio-temporal occurrence and their climatic triggers remains rather limited. Here, we present a dendrogeomorphic reconstruction of past flash flood activity in the Arroyo de los Puentes stream (Sierra de Guadarrama, Spanish Central System). We analyze a total of 287 increment cores from 178 disturbed Scots pine trees (*Pinus sylvestris* L.) which yielded indications on 212 growth disturbances related to past flash flood impact. In combination with local archives, meteorological data, annual forest management records and highly-resolved terrestrial data (i.e., LiDAR data and aerial imag-ery), the dendrogeomorphic time series allowed dating 25 flash floods over the last three centuries, with a major event leaving an intense geomorphic footprint throughout the catchment in 1936. The analysis of meteorological records suggests that the rainfall thresholds of flash floods vary with the seasonality of events. Dated flash floods in the 20th century were primarily related with synoptic troughs owing to the arrival of air masses from north and west on the Iberian Peninsula during negative indices of the North Atlantic Oscillation. The results of this study contribute considerably to a better understanding of hazards related with hydrogeomorphic processes in central Spain in general and in the Sierra de Guadarrama National Park in particular.

1. Introduction

Flash floods represent one of the most common natural hazards in mountain environments (Borga et al., 2008, 2014). The process is characterized by high flow velocities and important sediment charge causing severe damage and socio-economic losses, especially along the channels and on alluvial fans. In headwater catchments, torrential processes are moreover the main geomorphic agent responsible for landscape evolution (Carling, 1986; Foulds et al., 2014). From a scientific perspective, the understanding of the temporal dimension of these processes as well as their climatic triggers and subsequent effects on the environment are still a challenge worldwide, probably owing to the frequent occurrence of these processes in sparsely populated areas where archival data and systematic records are usually scarce (Mayer et al., 2010) or unrepresentative (Ayala-Carcedo, 2002). The lack of data on past activity therefore hampers the analysis of flash flood processes and calls for the use of alternative geomorphic approaches (Ibsen and Brunsden, 1996; Jakob, 2005). In this regard, paleohydrologic techniques allow to track the history of past (flash) flood events in ungauged catchments (Baker et al., 2002; Benito et al., 2003; Baker, 2008), and consequently, to improve links between process dynamics, climatic conditions and related hazards (Kingston et al., 2007; De Jong et al., 2009; Merz et al., 2014).

In mountain catchments, trees are frequently present next to torrential channels and on their banks, and can thus be used to reconstruct past flood activity with dendrogeomorphic methods (Stoffel et al., 2010). The systematic analysis of growth-ring series from trees disturbed by hydrogeomorphic processes (Stoffel and Wilford, 2012) typically yields valuable records of past events in ungauged mountain catchments with very high spatial and temporal accuracy (Shroder, 1980; Stoffel et al., 2010; Stoffel and Corona, 2014).

Dendrogeomorphical techniques have first been applied in fluvial geomorphology (Sigafoos, 1964; Sigafoos and Hendricks, 1961). However, despite that the utility of botanical evidence in paleohydrology has been recognized by many researchers (i.e. Baker, 1987; Hupp, 1988), tree rings have been used much less frequently as compared to other lines of evidence of paleofloods (e.g., slackwater deposits; Benito and Thorndycraft, 2004). The large potential of dendrogeomorphic tools for the assessment of frequency and magnitude of past events has been demonstrated in recent works (e.g., Ballesteros et al., 2011; Gottesfeld and Gottesfeld, 1990; Gottesfeld, 1996; Ruiz-Villanueva et al., 2010; Schraml et al., 2013; St. George and Nielsen, 2003). Further research has focused on changes in the spatial geomorphic patterns of processes (Arbellay et al., 2010; Bollschweiler et al., 2008; Stoffel et al., 2008) and on the seasonality and related climatic drivers of hydrogeomorphic processes (Schneuwly-Bollschweiler and Stoffel, 2012; Stoffel et al., 2011).

Here, we present a case study focusing on the spatio-temporal reconstruction of past flash flood activity in the Arroyo de los Puentes stream (Sierra de Guadarrama National Park, Spanish Central System). We analyze 178 Scots pine trees (*Pinus sylvestris* L.) disturbed by past flash flood events and couple this data with a large local historical forest management and climatic dataset of the study site to (i) report on the flash flood history of the stream during the last 212 years, and to (ii) identify local meteorological conditions which most likely acted as triggers of flash flood events during the past 83 years for which meteorological records exist locally.

2. Study site

The study site is located in the catchment known as *Arroyo de los Puentes* and its tributaries, located on the northern slope of the Guadarrama Mountains (Sierra de Guadarrama National Park, Spanish Central System, 40°47′37″N, 3°55′14″O; Fig. 1). The catchment covers approximately 2.5 km^2 and extends from the Bola del Mundo at 2258 masl to the alluvial fan area at 1500 masl. The average slope in the main channel is 9° (range: 7–18°).

The upper part of the catchment is occupied by extensive accumulations of unconsolidated gneissic materials prone to gelifraction. Water circulation in the source area is mostly subsuperficial, although several well-defined channels exist. The most characteristic geomorphic features in the central part of the catchment (between 1800 and 1600 masl) are linked with torrential activity, such as levees, lobes and well-defined avulsion channels. In this channel segment (at 1660 masl), Majabarca stream joins the main channel and exhibits several trees affected by floods. In the lower part of the catchment (from 1550 to 1480 masl) the valley opens and the gradient decreases, creating an alluvial fan at the confluence of Arroyo de los Puentes with Arroyo de las Pintadas stream. The fan covers an area of approximately 0.03 km^2 ha and its surface is crossed by several channels.

The region is dominated by a Mediterranean climate with continental influence that could be considered as ‘humid continental with warm summers’ (type ‘Dsb’: Köppen-Geiger classification, Peel et al., 2007). The study zone also has some Atlantic influence in the regime of rainstorms and is characterized by mild summers and long, cold winters. Average annual precipitation is 1326 mm with maximum rainfall in April, May, October, November and December (AEMET, 2011). Mean annual temperature is 6.5 °C at 1890 masl with mean monthly temperatures ranging from 2.9 °C in winter to 9.9 °C in summer, reaching up to 31.8 °C in August and −20.3 °C in December, as extreme values.

The study area is located in Montes de Valsaín (hereafter, Valsaín Forest), an extensive, managed *P. sylvestris* L. forest (10,700 ha). The forest is unique in the Mediterranean context owing to the extremely detailed record of forest management interventions started at the end of the 18th century and its management in general over more than eight centuries (Dones and Garrido, 2001).

3. Materials and methods

3.1. Geomorphic mapping and sampling strategy

A geomorphic characterization of all of the features related to hydrogeomorphic processes in the studied catchment was carried out by combining aerial imagery (cell size: 0.25 m), LiDAR data (cell size: 1 m) and field surveys. All geomorphic features were digitized using ArcGIS™ version 9.3 (ESRI, Redlands, CA, USA, 2009). Disturbed trees – namely wounded, tilted, decapitated or buried trees – located along the channel banks and/or on the fan were sampled following standard procedures in dendrogeomorphic studies as described in Stoffel and Corona (2014). Trees with possible disturbances by any process other than hydrogeomorphic (such as rockfall or human activities) were not been included in analysis. Trees were sampled with increment borers and two increment cores per tree were extracted with sampling positions being chosen according to the nature of the disturbance (Stoffel et al., 2005a). Samples were taken at the contact between the scar edge and the intact wood tissue to make sure that the entire tree-ring record was obtained (Schneuwly et al., 2009a,b). In parallel, undisturbed trees were also sampled in the upper and lower parts of the catchment to build a reference chronology and to identify pointer years for a reliable and precise cross-dating with disturbed trees (Touchan et al., 2013). Tree-ring widths were converted into width indices by standardizing raw data using ARSTAN software (Cook, 1985).

3.2. Tree-ring analysis and flash flood chronology reconstruction

Samples were prepared and measured following standard dendrochronological procedures (Stoffel and Corona, 2014). Individual growth series were obtained for each tree and cross-dated with the reference chronology, both visually and through statistical procedures (Stoffel et al., 2005a,b). Signatures of past flash flood activity were then identified on the increment cores and included injuries, callus tissues, compression wood, abrupt growth increase and/or growth suppression. Because *Pinus* spp. do not form tangential rows of traumatic resin ducts (or TRD, Stoffel, 2008), the seasonality of flash flood events had to be based on the position of wound borders within the increment rings.

For the separation of flood signals from noise related with other external processes affecting trees, we applied the weighted index value (W_{it}) as defined by Kogelnig-Mayer et al. (2011). This index considers the number and the intensity of growth disturbances (GDs) within each tree-ring series and the total number of trees available for the flash flood reconstruction. The W_{it} is calculated for each year of the reconstruction and considers differences in the intensity of tree reactions to mechanic disturbance related with past events. We screened recent publications to define appropriate thresholds for the identification of past hydrogeomorphic events (Corona et al., 2014; Schneuwly-Bollschweiler et al., 2013; Stoffel et al., 2011). In addition to the thresholds, we also visually analyzed the spatial distribution of the affected trees along the

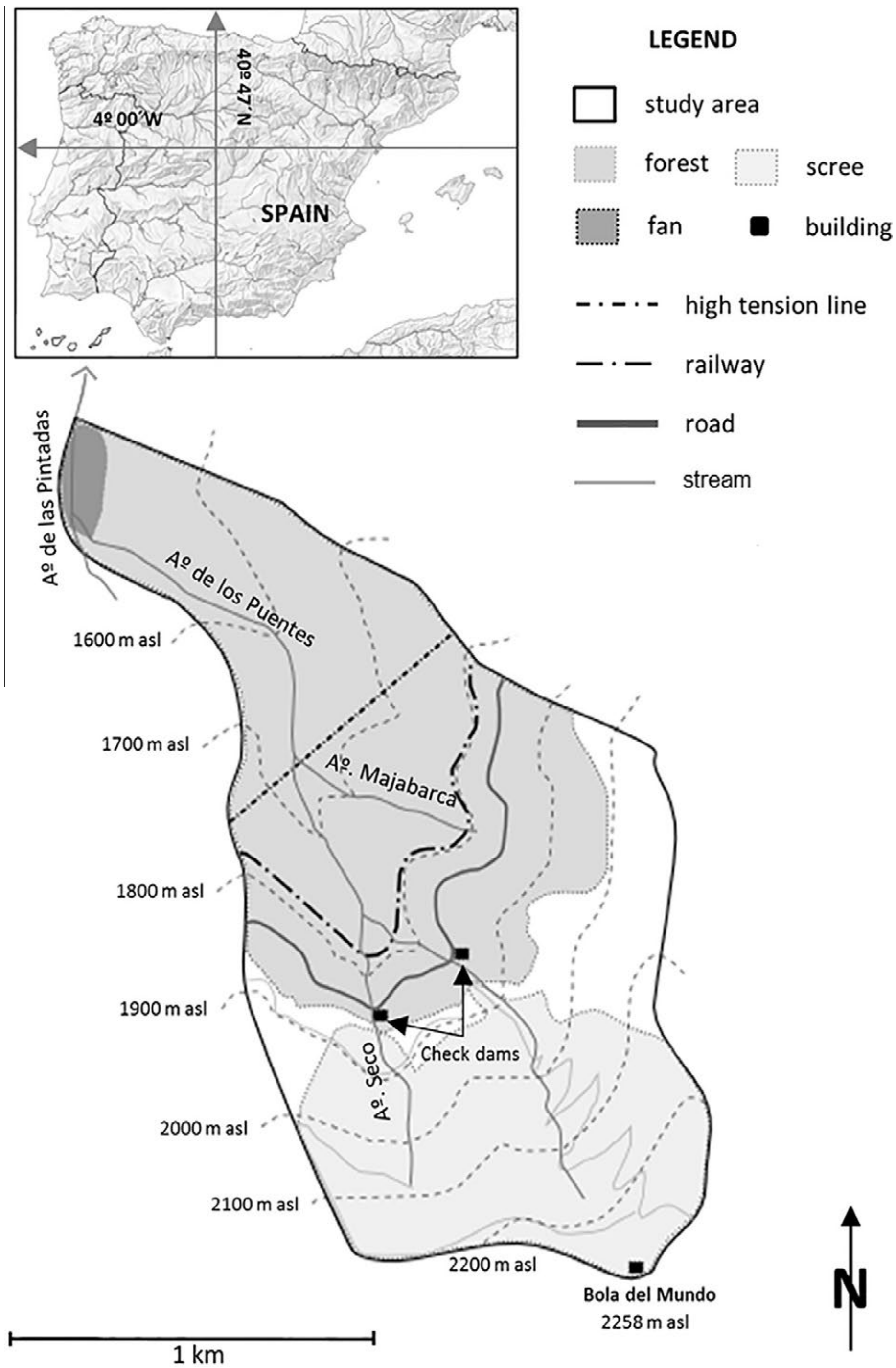

Fig. 1. General scheme of the study area showing the distribution of the anthropogenic elements with respect to the main streams.

channel and their relationship with geomorphic features (Lopez-Saez et al., 2011).

Owing to the fact that the anthropogenic influence in the Valsaín Forest is far from being negligible, we also took account of the very detailed and precise official register of forestry works carried out in the catchment since 1940. This additional information allowed discarding doubtful signals in years when intense forestry interventions were realized in the sampled area. Consequently, criteria to define flash flood events was defined as follows:

- $W_{it} > 1$: EVENT.
- $1 > W_{it} > 0.5$ without forestry work at the study area and more than 3 GDs: EVENT.
- $1 > W_{it} > 0.5$ with forestry work at the study area: NO EVENT.
- $W_{it} < 0.5$: NO EVENT.

3.3. Hydrometeorological analysis of reconstructed flash floods

Different historical archives have been screened to refine the (sub-) annually reconstructed dates of flash floods to the month or even the exact date. The sources analyzed included the archives from the Valsaín Forest documentary centre, national and local newspapers, local literature and meteorological ephemerides from the Spanish Meteorological Agency (AEMET). For those events in which a precise dating was not possible, we considered all potential triggering situations with the highest (or majors) rainfall precipitation totals (>30 mm) recorded throughout the year, but we also considered potential rain-on-snow processes. Subsequently, 1-, 3-, and 5-day cumulated rainfall totals were analyzed to determine the meteorological characteristics related with flash flood events at the study site. We also evaluated the monthly North Atlantic Oscillation Index (NAO) and synoptic situations prevailing before the occurrence of events.

Hydrometeorological data exists at Navacerrada, a meteorological station located next to the source area of the study site (40°47′N, 4°00′W, 1894 masl; Fig. 1) for the period 1933–2011. In addition, we consulted the time series from Segovia's meteorological station (40°56′N, 4°10′W, 1005 masl) for which daily data are available since 1894 (AEMET, 2011). Finally, for the definition of the large scale atmospheric flow and weather circulation patterns related with the reconstructed flash flood events, the Hess and Brezowsky Grosswetterlagen (GWL) weather classification system (Gestengabe and Werner, 2005; Parajka et al., 2010) was used. This catalogue provides daily information of patterns over Europe for the period 1881–2004, based on the mean air pressure distribution at both, surface level and 500 hPa level. In this study, we focused on 29 weather types classified into six different groups (Gestengabe and Werner, 2005; Parajka et al., 2010):

1. Zonal West: WA, WZ, WS, WW.
2. Mixed: SWA, SWZ, NWA, NWZ, HM, BM.
3. Mixed Central Europe (CE): TM.
4. Meridional North (N): NA, NZ, HNA, HNZ, HB, TRM.
5. Meridional Northeast and East (NE, E): NEA, NEZ, HFA, HFZ, HNFA, HNFZ.
6. Meridional Southeast and South (SE, E): SEA, SEZ, SA, SZ, TB, TRW.

4. Results

4.1. Age structure of the forest stand

The reference chronologies developed for the upper and lower parts of the study area covered the periods 1784–2011 and 1748–2011, respectively. The tree-ring growth indices showed for both sites narrow rings in 1829, 1889, 1950, 1972, 1986 and 1996 (Fig. 2). These narrow rings were used for the visual cross-dating of reference trees (undisturbed) with disturbed trees. Data on the pith age at breast height indicated that the 178 trees sampled at Arroyo de los Puentes stream were on average 150 years old (±77 years). The oldest tree selected for analysis attained sampling height in 1680, whereas the youngest tree reached sampling position in 2000. At least 37 trees were living in 1800, hence the time period considered is well represented by the sampled depth.

4.2. Flash flood reconstruction

A total of 212 GDs were identified in 287 increment cores, most of them in the form of scars ($n = 91$, 42%). Among the other types of GDs, we observed 50 occurrences of reaction wood (23%), 42 trees exhibited an abrupt growth suppression ($n = 42$, 19%), whereas growth releases ($n = 18$, 8%) and callus tissues ($n = 11$, 5%) were much less frequent. From all GDs, 43% were classified as very strong, 34% as intermediate and 23% as weak reactions.

Based on the number and intensity of reactions as well as the sample depth available for each year of the reconstruction, Fig. 3 shows the computed W_{it} index, which ranks between 0.04 and 36.3. In 28 years, the W_{it} index exceeded the combined threshold of $W_{it} > 0.5$ and GDs $\geqslant 3$ (Table 1). The historical forest

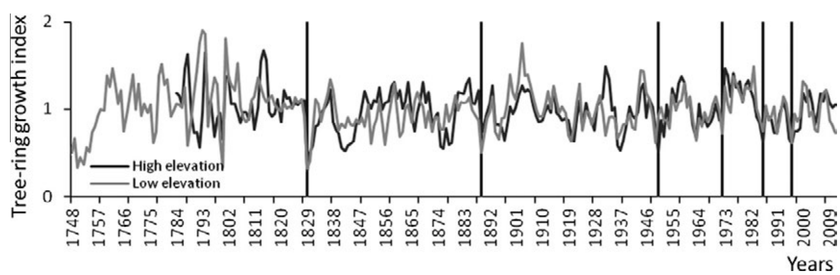

Fig. 2. Reference chronologies of *Pinus sylvestris* L. for Arroyo de los Puentes stream, obtained at the high and low-elevation parts of the catchment; the series cover the periods 1784–2011 and 1748–2011, respectively. Individual series were standardized and indexed. The vertical black lines indicate years characterized by narrow rings in both series (1829, 1889, 1950, 1972, 1986 and 1996).

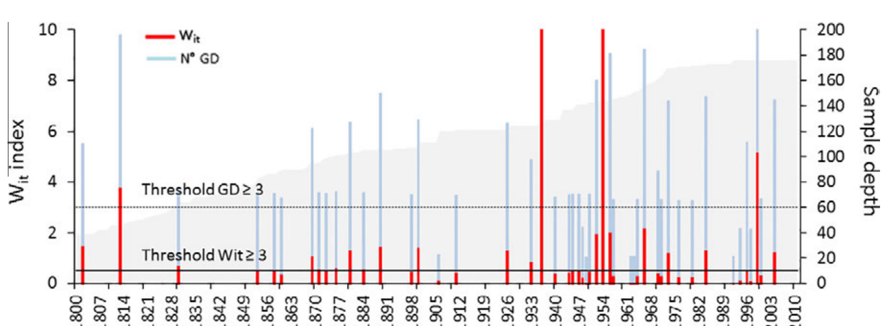

Fig. 3. Event-response histograms showing flash-flood induced growth responses from the sampled *Pinus sylvestris* L. trees. Blue lines show the total number of growth disturbances (N° GDs), whereas the red lines indicate the percentage of trees responding to an event based on the weighted index value (W_{it}) of Kogelnig-Mayer et al. (2011) (In 1936 the $W_{it} = 36.38$; in 1954 $W_{it} = 10.98$). The horizontal lines denote the GDs (dotted line) and W_{it} (solid line) thresholds used for the reconstruction of past events whereas the gray shade in the back indicates the sample depth, i.e., the number of trees available for analysis in a specific year. (For interpretation of the references to color in this figure legend, the reader is referred to the web version of this article.)

Table 1
Intensity reactions, n° of growth disturbances (GDs) and W_{it} value for each event assessed.

Years	Sample depth	Growth disturbance			N° GDs	W_{it}
		High intensity	Medium intensity	Weak intensity		
1802	34			4	4	1.50
1813	41	1	1	4	6	3.79
1830	59	1		2	3	0.70
1853	75	1		2	3	0.57
1858	78	1		2	3	0.54
1869	84		1	4	5	1.10
1871	85		3		3	0.58
1874	89		3		3	0.55
1876	90		3		3	0.54
1880	92		4	1	5	1.34
1884	94	1	2		3	0.57
1900	100	2	2	1	5	1.44
1906	109	1	2	1	4	0.73
1926	111	2	3		5	1.31
1933	111	3		1	4	0.86
1936	112	19	6		25	36.38
1945	120	3			3	0.53
1947	124	3			3	0.51
1950	126	3			3	0.50
1952	127	6			6	1.98
1954	127	12		3	15	10.98
1956	127	3	2	2	7	2.04
1966	137	4	3		7	2.20
1973	149	1	4	1	6	1.21
1984	152	2	4		6	1.34
1996	155		1	4	5	0.55
1999	155	9	2		11	5.18
2004	155	1	5		6	1.24

Table 2
Match between forestry actions, reasons for the works and responses in trees. Gray shading highlight years in which reconstructed disturbances in trees match with forestry work. Letters indicate the causes of the felling of trees during forestry actions in the catchment (E-extraordinary, R-regular, D-dead trees and I-insects).

Year	Sample depth	Growth disturbance			W_{it}	Cause
		High intensity	Medium intensity	Weak intensity		
1940	112		3	0	0.40	R
1945	120	3	0	0	0.53	E
1950	126	3	0	0	0.50	E
1962	130	1	0	0	0.05	R
1972	149	0	3	0	0.30	D
1996	155	0	1	4	0.55	E
2000	155	2	0	1	0.33	E and I

management database indicated that the sampled area, divided into five forest management units, was subjected to periodically forestry interventions, starting in the early 1940s. Table 2 shows the match between forestry activities as well as the reasons for the interventions. At least 3 years (1945, 1950, and 1996), categorized as potential flood events in Table 1, match with years of forestry interventions following "extraordinary events" in the study reach. In the case of 1945 and 1996, these "extraordinary events" were related to large snow falls which provoked widespread forest damage; but the nature of the extraordinary 1950 event is unknown.

As a consequence of these records, the reconstructed flash flood chronology has been reduced to 25 reconstructed events at the study site. The most significant events, in terms of threshold values with a $W_{it} > 5$, took place in 1936 ($W_{it} = 36.3$), 1954 ($W_{it} = 10.9$) and 1999 ($W_{it} = 5.18$). In addition, three years showed events with indices ranging from $5 \geqslant W_{it} \geqslant 2$, these were in 1813 ($W_{it} = 3.7$), 1966 ($W_{it} = 2.2$) and 1956 ($W_{it} = 2.0$). Nine years showed a W_{it} comprised between 1 and 2 (i.e., 1802, 1869, 1880, 1900, 1926, 1952, 1973, 1984 and 2004), whereas in 10 cases the W_{it} ranked between 0.5 and 1 (i.e., 1830, 1853, 1858, 1871, 1873, 1876, 1884, 1906, 1933, and 1947). Considering the flash flood activity in the Arroyo de los Puentes catchment since 1802, the reconstructed frequency was 0.12 events/year. The partial frequency increased in 1870s with 5 flash floods in 10 years and between 1940s and 1950s with 4 events between 1947 and 1956 (Fig. 4).

Fig. 5A illustrates the three main patterns of GDs distribution at the study site. During more than two-thirds of all events, GDs were limited to trees growing along the Arroyo de los Puentes stream, whereas disturbance signals were missing completely in its tributary (70% of all events, i.e., 1802, 1813, 1830, 1853, 1858, 1869, 1871, 1874, 1876, 1880, 1884, 1900, 1906, 1936, 1945, 1947, 1950, 1956, 1973, 1984, 1996 and 2004). In four cases (17%; 1926, 1933, 1966 and 1944), GDs were observed in the Arroyo de los Puentes and the Majabarca streams. In three cases (13%, i.e. 1952, 1954 and 1999) GDs were only recorded in Majabarca stream.

4.3. Hydrometeorological triggers and synoptic situation

The assessment of the seasonality of flash floods and/or the calendar-dating of reconstructed events was based on the intra-annual position of the damages in the tree-ring records, historical archives, contemporary newspaper reports, as well as on literature

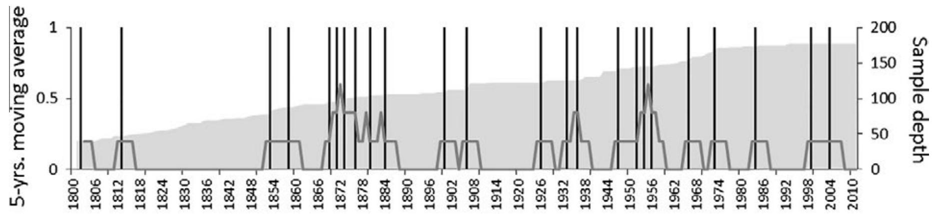

Fig. 4. Flash flood chronology and 5-year moving average obtained at Arroyo de los Puentes stream.

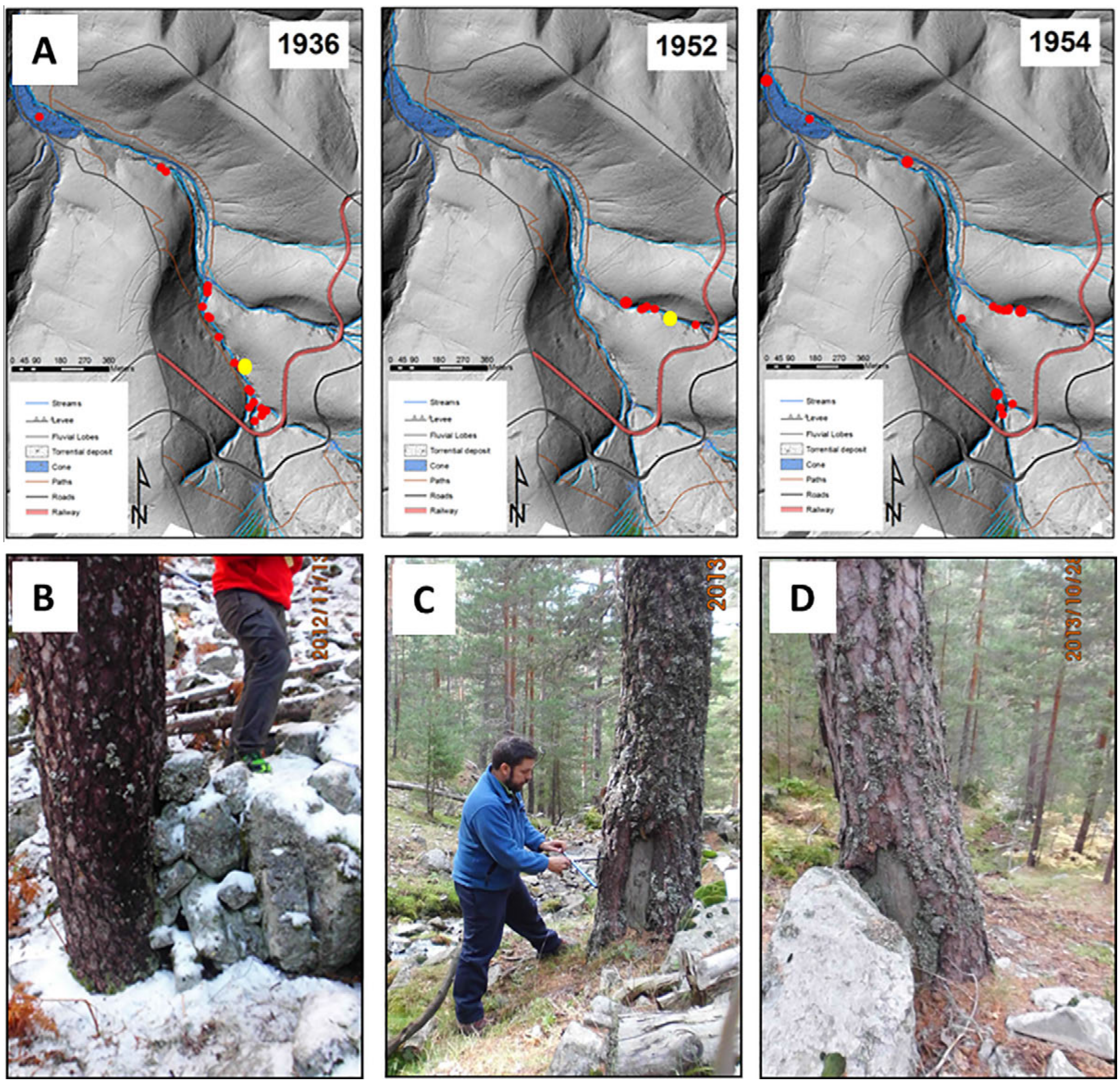

Fig. 5. Reconstructed patterns of past flash flood events. (A) Maps showing the location of trees present (black) at the moment of flash flood occurrence as well as those (red) showing a disturbance induced by the flash flood. Yellow dots are examples of trees impacted by the flash floods in 1936, 1952, and 1954: (B–D) sedimentation and scar associated with the 1936 event; (C and D) impact scar related with sediment transported during the flash flood events in 1952 and 1954, respectively. (For interpretation of the references to color in this figure legend, the reader is referred to the web version of this article.)

existing on flash floods in the wider study region. This approach allowed a realistic calendar-dating of seven 20th century flash floods (i.e., 1900, 1936, 1952, 1954, 1956, 1984 and 1999). By contrast, local documentation or indirect evidence of events could not be found for the events which occurred in 1906, 1926, 1933, 1947, 1966, 1973 and 2004.

In the case of the calendar-dated flash floods, Table 3 shows the main hydrometeorological variables analyzed as well as the distribution of events throughout the year. It becomes obvious that flash floods are mostly limited to the moist seasons with reconstructed flash flood events occurring mainly in autumn–winter (October 1900, February 1936, March 1952, November 1954, January 1956), and a unique flash flood in spring (May 1984) and another one during summer (September 1999). For events without exact monthly date (Table 4), the most likely seasonality were October–November (7 potential cases), May–April (5 potential

Table 3
Hydrometeorological triggers (in gray analysis based on Segovia station) related to reconstructed events matching with historical archives.

Year	Date	Temp °C (max/min)	Rainfall 1-day	Rainfall 3-day	Rainfall 5-day	NAO-index	GWL system	References/Newspaper/indicator
1900	13/10	15°/7°	73	123	123	−0.57	WZ	La Vanguardia-14/10/1900-pp2
1936	29/02	5°/–°	36	47	91	−2.44	TM	Seasonality based on anatomical interpretation
1952	31/03	–°/1.3°	101.8	143.5	276.9	−1.14	HNZ	El Adelantado de Segovia-01/04/1952
1954	8/11	5.8°/5°	55	145.7	149.3	1.54	WZ	ABC-07/11/1954-pp 039
1956	18/01	–°/1.2°	39	104.2	112.1	−0.76	NWZ	Díez Herrero et al. (2008)
1984	14/05	2.2°/–°	27	38.5	38.5	−2.34	HFZ	Morales and Ortega (2002)
1999	18/09	12°/7°	27	27.3	35.8	−0.54	TRW	Seasonality based on anatomical interpretation

Table 4
Potential hydrometeorological triggers (in gray analysis based on Segovia station) related to reconstructed events not recorded on historical archives.

Year	Date	Rainfall 1-day	Temp °C (max/min)	Rainfall 3-day	Rainfall 5-day	NAO-index
1906	12/05	27	15°/6°	39	79	−1.75
	12/11	30	8°/5°	49	64	0.7
1926	23/10	27	17°/2°	52	52	−4.16
1933	20/04	40	5°/3°	40	40	−0.23
	9/10	54 (12 h)	–°/3°	54	54	−2.03
	21/10	74 (12 h)	10°/0°	82	82	−2.03
1947	05/03	40	6.4°/1°	57	92	−1.2
1966	03/10	104.9	9.2°/9°	132.5	136	−2.89
	07/11	94.7	0.8°/0.2°	302.5	321.1	−0.07
1973	05/11	46.7	6°/3.8°	141.5	162.8	−0.26
	03/05	30.2	4°/0.6°	73.6	73.6	0.37
	19/05	41.6	3°/0°	106.8	128.7	0.37
2004	23/05	31	10.2°/6.6°	49.5	49.5	0.19

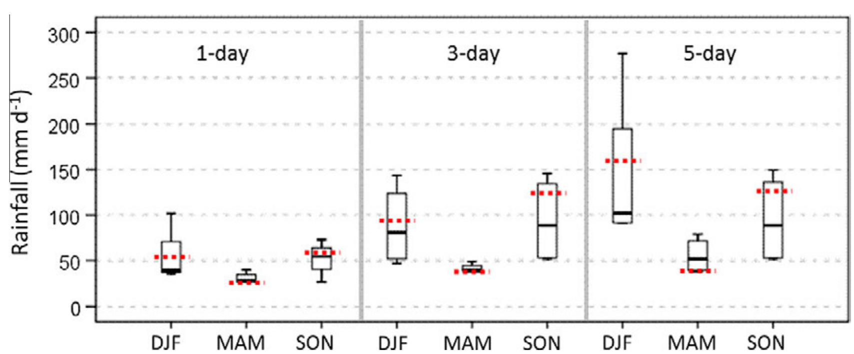

Fig. 6. One-day, 3-day and 5-day average rainfall thresholds related to reconstructed events according to the likely seasonal correspondence. Red lines indicate average rainfall thresholds corresponding with events contrasted by historical archives. In summer season, we only found one event (1999) characterized by a 1-day rainfall threshold of almost 27 mm, 3-day of 27.3 mm and 5-day of 35.8 mm, respectively. Seasonality: winter (22nd-December to 22nd-March); spring (23rd-March to 22nd-June); and autumn (23rd-September to 21st-December). (For interpretation of the references to color in this figure legend, the reader is referred to the web version of this article.)

cases) and March (1947). With exception of only two cases (1954 and 2004), all the events were related to a negative monthly NAO-index.

Analysis of rainfall thresholds related with the likely triggers of reconstructed events (period with available data: $n = 14$) showed differences in precipitation which can likely be related to the seasonality of storms (Fig. 6). Despite the small sample used for analysis, we observed that autumn and winter flash floods were clearly characterized by higher rainfall totals than those occurring in spring or summer. The thresholds for winter events were 54.2 mm, 87.7 mm, and 143.0 mm for the largest 1-, 3-, and 5-day rainfall, respectively. Spring flash floods were characterized by rainfall thresholds of 32.4, 56.6, and 67.6 mm for the same durations, whereas events in autumn had thresholds of 67.9, 139.8, and 146.6 mm for the largest 1-, 3-, and 5-day rainfall totals, respectively. For the case of the unique summer event (1999), the triggering rainfall showed totals of 27, 27.3, and 35.8 mm for the 1-, 3-, and 5-day rainfall, respectively. The very small 1- and 3-day rainfall totals recorded at Navacerrada station located next to the source areas of flash floods may point to a short-lived, but intense storm as the trigger of the flash flood.

The GWL weather classification system and analysis of the isobaric maps at 500 hPa and surface level associated with the precipitation records triggering the identified events suggested different weather patterns (Fig. 7). Meridional patterns were identified in three cases (i.e. 1952, 1984 and 1999), whereas zonal patterns were observed in two cases (i.e. 1900 and 1954). Two more cases showed a deep low pressure system in Europe (i.e. 1936) and a mixed pattern affected by a north-west air masses (i.e. 1956). Therefore, the identified meteorological causes probably related to the reconstructed events are the following: frontal systems (69% of cases), combination of frontal systems and snowmelt processes (23% of cases) and convective storms (8% of cases), respectively.

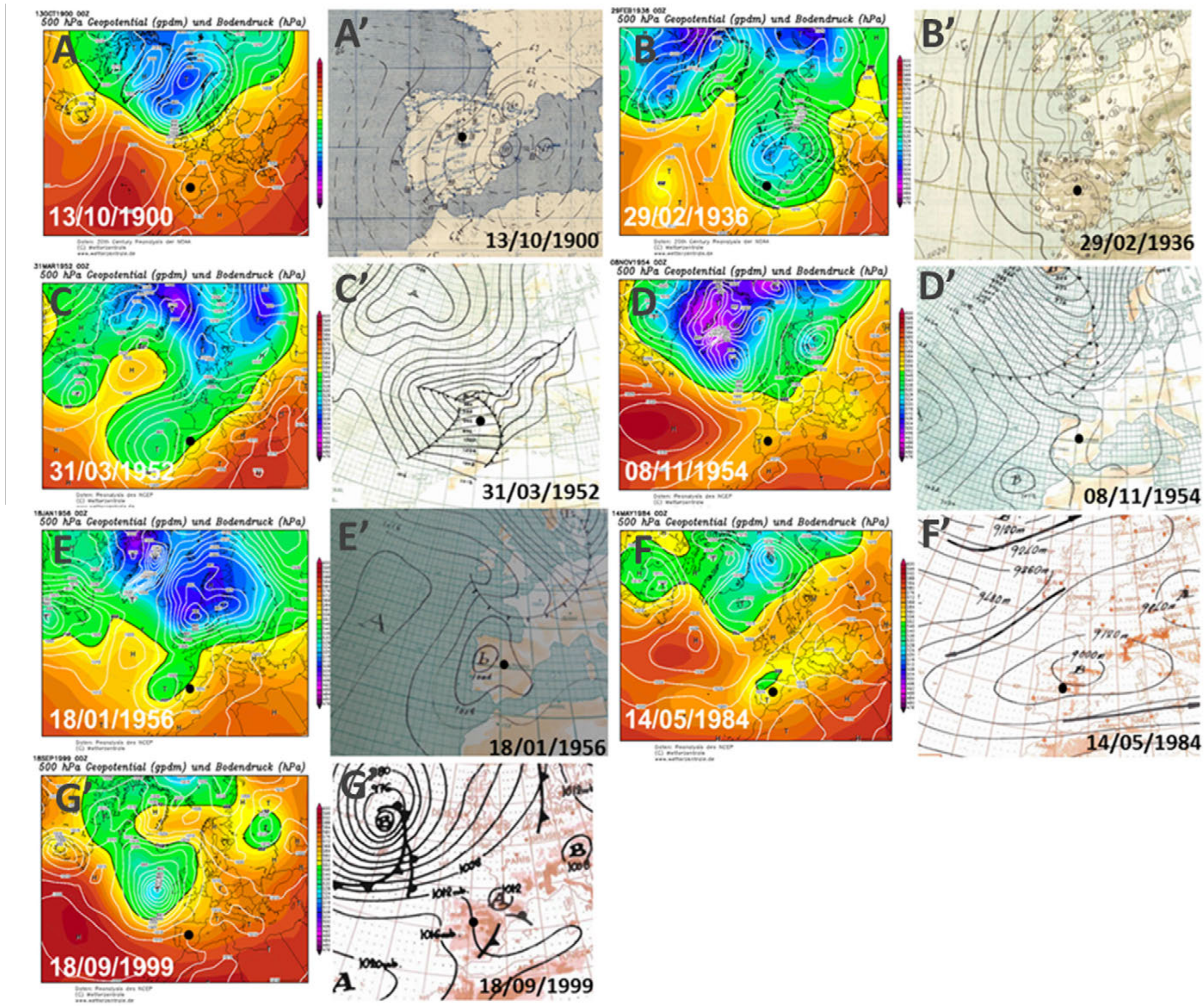

Fig. 7. Synoptic situation (at surface level and 500 hPa level) related with dated flash flood events at the central part of Spain: (A 500 hPa level; A' surface level-hereafter)) 13/10/1900 (WZ): zonal atmospheric circulation with low air pressure on the east of the Iberian Peninsula – advection at the study site W; (B) 29/02/1936 (TM) Mixed Central Europe, depth low air pressure on France – advection N; (C) 31/03/1952 (HNZ) meridional atmospheric circulation with depth low air pressure on the NW of the Iberian Peninsula – advection NW; (D) 08/11/1954 (WZ) zonal atmospheric circulation with a trough on the Iberian Peninsula, polar air masses – advection NW; (E) 18/01/1956 (NWZ) mixed atmospheric circulation with a trough on the Iberian Peninsula – advection W; (F) 14/05/1984 (HFZ) meridional atmospheric circulation with low pressure on the Iberian Peninsula, Atlantic air masses – advection N; (G) 18/09/1999 (TRW) meridional atmospheric circulation with a depth low pressure on Britain, Atlantic air masses – advection W. Maps from http://www.wetterzentrale.de (500 hPA, NCEP Reanalysis data) and the Spanish Meteorological Agency (surface maps; http://www.aemet.es/es/conocermas/fondos_digitales/boletines).

5. Discussion

In this study we provide a 212-year chronology of flash floods based on tree-rings reconstructions performed in the ungauged Arroyo de los Puentes catchment located in the Sierra de Guadarrama National Park (Spanish Central System) and characterize the meteorological triggers of those past flash floods. We report results derived from the analysis of 287 increment cores of 178 living *P. sylvestris* L. trees. The growth-ring records of these trees allowed the detection and dating of 212 GDs attributed to 25 flash flood events which occurred since 1802.

The reconstructed flash flood chronology complements the existing flood record for the contributing highland catchment of the Eresma River and represents the longest and most continuous (annually-resolved), non-systematic record of flash flood activity and related climatic factors in this area. Results are therefore expected to greatly support the definition of flash flood hazard zones in an area characterized by intense tourist activity (e.g., the recently founded Sierra de Guadarrama National Park) and by a concentration of linear transport infrastructures (i.e. railway lines, roads, power lines and hiking paths).

Our reconstruction points to a flash flood frequency of 0.12 events/year in the Arroyo de los Puentes stream for the last 212 years. Individual event years match with the chronology of recorded (i.e., gauged) flood events in the Eresma River. We have successfully identified evidences of the two major lowland floods of 1956 and 1966 in the trees from one of the contributing highland catchments. Moreover, existing archives and local contemporary newspapers reports provide further evidence for extreme hydroclimatic conditions in the Eresma River and other parts of central Spain in 1936, 1956, 1966, 1984, and 1996 (see Table 5). These years also appear, without any exception, in the dendrogeomorphic flash

Table 5
Correspondence between reconstructed flash flood events at Arroyo de los Puentes stream and information about flood events in central Spain.

Years	N° GDs	W_{it}	References	Date	Selection of historical facts related with floods in central Spain
1802	4	1.50	–	–	–
1813	6	3.79	–	–	–
1830	3	0.70	Potenciano (2004)	1/9/1830	Floods in Tagus and Jarama Rivers
1853	3	0.57	Ruiz-Villanueva et al. (2013)	–	Floods in Tagus basin
1858	3	0.54	Morales and Ortega (2002)	–	Strong damages in Fuentes Village because of overflows of the Duero river
1869	5	1.10	Potenciano (2004)	–	Tagus basin
1871	3	0.58	–	–	–
1874	3	0.55	–	–	–
1876	3	0.54	Benito et al. (2003a)	December	Floods and overflows in The Tagus and Jarama rivers in the Central and Southern sectors of the Iberian peninsula
			Benito et al. (2003b) Trigo et al. (2014) Potenciano (2004)		
1880	5	1.34	–	–	–
1884	3	0.57	–	–	–
1900	5	1.44	Morales and Ortega (2002)	11/2/1900	Floods in Duero basin affecting to important cities like Salamanca, Soria, Burgos and Leon
1906	4	0.73	–	–	–
1926	5	1.31	Potenciano (2004)	November	Tagus basin
1933	4	0.86	–	–	–
1936	25	36.38	Ruiz-Villanueva et al. (2013) Morales and Ortega (2002) Potenciano (2004) Benito et al. (2003b)	Between January and February	Several tributary streams of the high Tagus catchment and Arenal river in Gredos, suffer important floods. Towns along these streams are affected (e.g. Guadalajara, Aranjuez, Alcalá de Henares in the central Spain and Guisando and Candeleda in Gredos. The same occurs in the Duero basin affecting to Esgueva (Valladolid)
1945	3	0.53	–	–	–
1947	3	0.51	Ruiz-Villanueva et al. (2013) Morales and Ortega (2002) Benito et al. (2003a) Benito et al. (2003b) Trigo et al., 2014	–	Tagus and Duero basins
1950	3	0.50	–	–	–
1952	6	1.98	–	–	–
1954	15	10.98	–	–	–
1956	7	2.04	Díez Herrero et al. (2008) Morales and Ortega (2002) (Potenciano, 2004)	January and March	20.01.1956, floods in Eresma river affecting to Segovia city. Also in January references to floods in Jarama and Manzanares rivers close to Madrid city. In March, references to generalized floods
1966	7	2.20	Ruiz-Villanueva et al. (2013) Díez Herrero et al. (2008)	29/03/1966	Flood in Eresma river affecting to Segovia city. Dendrogeomorphic evidence was clearly visible in trees in Gredos area
1973	6	1.21	Potenciano (2004) Ruiz-Villanueva et al. (2013)	–	Overflows in Alberche river (tributary of Tagus) affecting to Pepino village in Toledo. Also dendrogeomorphic evidence for this year in Gredos area
1984	6	1.34	Ruiz-Villanueva et al. (2013)	15/05/1984	Flood in Eresma river. Also references to floods in Tagus basin in this year (unknown date). Dendrogeomorphic evidence of floods in Gredos in this year
			Morales and Ortega (2002) Benito et al. (2003a)		
1996	5	0.55	Ruiz-Villanueva et al. (2013) Díez Herrero et al. (2008)	23/01/1996	Floods cause of snowmelt in Eresma catchment
			Morales and Ortega (2002) Benito et al. (2003a)		Also references to floods in Tagus basin
1999	11	5.18	Ruiz-Villanueva et al. (2013)	12/07/1999	In July floods in the center area affecting towns and villages (Valladolid, Navas del Marqués and Vinuesa). In September floods in Voltoya river (Duero basin) and thunderstorm in the central mountain range
			Morales and Ortega (2002)	01/09/1999	
2004	6	1.24	–	–	–

flood reconstruction in the Arroyo de los Puentes stream, and thereby indirectly confirm the robustness of the time series reconstructed in this study.

Our results showed two periods with intense flash flood activity between 1870 and 1884 and between 1947 and 1956. On the basis of historical literature from the 19th century, the first period with very frequent flash floods can be related to meteorological anomalies characterized by significant oscillations in atmospheric pressure, high snow cover in winter and an excessive number (103) of intense precipitation events including storms (Breñosa and Castellarnau, 1884). The reconstruction from Arroyo de los Puentes is in agreement with observations from the Tagus basin (central Spain) where Benito et al. (2003a,b) observed a similar increase in the frequency of flood events. The most intense event was detected in 1936 (W_{it} = 36.38 and GDs = 25). This observation is also in agreement with other studies in the Spanish Central System (Potenciano, 2004; Ruiz-Villanueva et al., 2013), and hence confirm the extraordinary nature of this flash flood.

In methodological terms, the preferred use of the W_{it} index value (Kogelnig-Mayer et al., 2011) – instead of the Shroder index (Shroder, 1980) – was not only justified by the large amount of flood scars found in the trees along the channel (42%), but also was needed in view of the hypothetical influence of intense forest management on accidental growth anomalies in trees. The preferential weighting of strong signals (i.e., flood scars), as suggested by Stoffel and Corona (2014), did not only filter low-frequency noise in the time series more efficiently, but also yielded a reconstruction for which local flash flood events seem to converge with the dates of regional floods. Despite the convincing match between local flash floods and regional flood events, it is necessary to emphasize that dendrogeomorphic reconstructions of past geomorphic activity (of any nature) will always remain as minimum frequencies (Bollschweiler et al., 2011). Therefore, some events could remain missed even if efforts are undertaken to optimize sample depth to minimize noise and to maximize signals (e.g., Corona et al., 2012, 2013, 2014; Schneuwly-Bollschweiler et al., 2013; Stoffel et al., 2013). This assertion is further underlined by the fact that internal scars (i.e., blurred or hidden injuries which can no longer be seen on the stem surface) cannot be detected easily in *P. sylvestris* L., as this species – unlike other conifers – does not form TRD around wounds (Stoffel, 2008), thus hampering the indirect dating of scars with seasonal precision (Stoffel and Hitz, 2008). Our study is also limited by the fact that we were unable to show the occurrence of repeated flash floods in the same year (Schneuwly-Bollschweiler and Stoffel, 2012).

Analysis of hydrometeorological triggers was based on 14 flash floods covering the span of the available precipitation records. The period of flash flood occurrence could be narrowed down in 7 out of 14 cases using historical archives and/or the intra-seasonal position of scars in trees. In 1956 and 1966, the exact date of events has been documented and could thus been used directly. The intra-annual position of injuries was most helpful for the precise dating of the 1936 and 1999 events. For the remaining events we used newspaper reports and local archives (see above). In case that the seasonality of flash floods was known, we assumed that events were triggered by the greatest rainfall recorded within the time window suggested by the intra-annual position of scars in trees and/or by archival records (Schneuwly-Bollschweiler and Stoffel, 2012). For the 6 remaining cases, neither direct nor indirect references to floods or intense rainfalls could be found, so that the analysis of potential triggers was extended to the entire year. As a result of the proximity of the Navacerrada station (only 900 m away from the source area of flash floods and located at a similar altitude) and the good quality of the data, the climate dataset analyzed in this study is highly reliable. Because the resolution of the precipitation time series was daily (and not hourly), we could not perform an intensity–duration–frequency (IDF) analysis for each event, but still believe that the obtained 1-, 3-, and 5-day rainfall thresholds presented in this study are reliable enough to understand average rainfall thresholds involved in the triggering of flash floods at the study site (Kundzewicz et al., 2014).

Our results suggest that daily rainfall threshold strongly depend on the season of flash floods. In that sense, flash floods occurring in spring were typically related to lower rainfall totals as compared to flash floods in autumn and winter. This observation also clearly points to the predominant role of snowmelt processes and soil moisture structure triggering flash floods in winter and spring (De Jong et al., 2009), confirming the conclusion provided by Marchi et al. (2010). In the case of the largest event on record (1936), we also demonstrate that, depending on the seasonality of flash floods, events will not necessarily be triggered by the most important hydrometeorological event and/or the largest precipitation recorded during a year. The time series presented in this study also highlight the importance of independent, seasonal flood-frequency analyses to obtain reliable flood hazard assessments (Baratti et al., 2012; Merz et al., 2014).

At the study site, flash flood events typically took place between autumn and spring, which is in agreement with findings from Ruiz-Villanueva et al. (2013) who obtained similar conclusions for headwater catchments in the western part of the Spanish Central System. The main synoptic situations related with the triggering of flash floods were cold Atlantic and continental air masses transported to the study site by low pressure systems generating synoptic troughs over the Iberian Peninsula (Tomás et al., 2004). In 84% of the cases, flash floods were related to negative monthly NAO indices, showing in six cases moderate to intense negative values (with NAO < -1). Our observations are in agreement with results from other mountain catchments in central Spain (e.g., Benito et al., 2003a,b, 2005, 2008) and support the idea that intense hydrometeorological activity in central Spain is related to the antecedent NAO mode (Cortesi et al., 2012; Salgueiro et al., 2013; Trigo et al., 2004). The weather circulation patterns related with flash floods dated in this contribution confirm the casuistry associated with flash flood events in the study area, which was slightly weighted toward Meridional circulation patterns. The mixed Central European (TM) pattern was in addition responsible in the triggering of the most intense event defined in this study. Our results are confirmed by observations obtained by Parajka et al. (2010) who related Meridional circulation patterns with precipitation events and related floods in northern Italy. However, the lower number of event defined in this study is presumably due to the nature of this study (local catchment rather regional study) and thus avoids to draw robust conclusions in this regard.

6. Conclusions

Flash flood activity in the Arroyo de los Puentes catchment (northern slope of Sierra Guadarrama) was reconstructed during the last 212 years using GDs from a large number of disturbed trees (*P. sylvestris* L.). The reliability of the presented flash-flood chronology was, therefore, supported by a large climatic and historical forest dataset. Despite the potential limitation related with the use of indirect proxies, this study is supporting the usefulness of the dendrogeomorphic approach for the understanding of past climate-floods in managed mountain areas. Our results describe the complexity of processes in the catchment, as both snowmelt and soil humidity have a major role as triggers of past geomorphic events. In addition, we detected that periods with more intense and frequent flash flood activity were related to negative NAO phases. Therefore, this study provide crucial data to gain a better understanding about the spatio-temporal patterns of flash flood occurrence and their links with climate in the Sierra de Guadarrama National Park.

Acknowledgments

This study has been partially funded by the projects IDEA-GesPPNN-163/2010 (OAPN – Organismo Autónomo de Parques Nacionales, Ministerio de Agricultura, Alimentación y Medio Ambiente) and CGL2010-19274 (projects MAS Dendro-Avenidas) of the Spanish Ministry of Economy and Competitiveness. The authors sincerely acknowledge Marco Borga and other anonymous reviewer. Special recognition must be given to CENEAM, Montes de Valsaín, OAPN and JCyL for providing information for this study. Specifically, they want to thank Javier Donés (Director of Montes de Valsaín), Ramzi Touchan and Dave Meko for their support during the study, as well as Andrés Díez and Gerardo Benito and all participants of the *Tree-ring summer school* carried out in 2012 in Valsaín (Touchan et al., 2013). R. Sánchez-Salguero thanks the financial support from University of Córdoba-Campus de Excelencia Internacional-ceiA3.

AEMET, 2011. Atlas climático ibérico. Agencia Estatal de Meteorología.
Arbellay, E., Stoffel, M., Bollschweiler, M., 2010. Dendrogeomorphic reconstruction of past debris-flow activity using injured broad-leaved trees. Earth Surf. Process. 35, 399–406.
Ayala-Carcedo, F.J., 2002. Análisis de riesgos por movimientos de ladera. In: Ayala-Carcedo, F.J., Olcina, J. (Eds.), Riesgos naturales. Ed Ariel, Barcelona, pp. 379–407.
Baker, V.R., 1987. Paleoflood hydrology and extraordinary flood events. J. Hydrol. 96, 79–99.
Baker, V.R., 2008. Paleoflood hydrology: origin, progress, prospects. Geomorphology 101, 1–13.
Baker, V.R., Webb, R.H., House, P.K., 2002. The scientific and societal value of paleoflood hydrology. In: House, P.K., Webb, R.H., Baker, V.R., Levish, D.R. (Eds.), Ancient Floods, Modern Hazards: Principles and Applications of Paleoflood Hydrology, Water Science and Application, vol. 5. Am. Geophys. U, Washington, D.C., pp. 1–19.
Ballesteros, J.A., Eguibar, M., Bodoque, J.M., Díez, A., Stoffel, M., Gutiérrez, I., 2011. Estimating flash flood discharge in an ungauged mountain catchment with 2D

hydraulic models and dendrogeomorphic paleostage indicators. Hydrol. Process. 25, 970–979.
Baratti, E., Montanari, A., Castellarin, A., Salinas, J.L., Viglione, A., Bezzi, A., 2012. Estimating the flood frequency distribution at seasonal and annual time scales. Hydrol. Earth Syst. Sci. 16, 4651–4660.
Benito, G., Thorndycraft, V.R., 2004. Systematic, palaeo-flood and historical data for the improvement of flood risk estimation. CSIC, Madrid.
Benito, G., Sopeña, A., Sánchez-Moya, Y., Machado, M.J., Pérez-González, A., 2003a. Palaeoflood record of the Tagus River (central Spain) during the Late Pleistocene and Holocene. Quat. Sci. Rev. 22, 1737–1756.
Benito, G., Díez-Herrero, A., Fernández De Villalta, M., 2003b. Magnitude and frequency of flooding in the Tagus basin (central Spain) over the last millennium. Clim. Change 58, 171–192.
Benito, G., Barriendos, M., Llasat, C., Machado, M., Thorndycraft, V., 2005. Impactos sobre los riesgos naturales de origen climático. Riesgo de crecidas fluviales, In: Moreno, J.M. (Eds.), Evaluación preliminar de los impactos en España por efecto del cambio climático. Proyecto ECCE – Informe final. Ministerio de Medio Ambiente, Madrid, pp. 525–548.
Benito, G., Thorndycraft, V.R., Rico, M., Sánchez-Moya, Y., Sopeña, A., 2008. Palaeoflood and floodplain records from Spain: Evidence for long-term climate variability and environmental changes. Geomorphology 101, 68–77.
Bollschweiler, M., Stoffel, M., Schneuwly, D.M., 2008. Dynamics in debris-flow activity on a forested cone – a case study using different dendroecological approaches. Catena 72, 67–78.
Bollschweiler, M., Stoffel, M., Schläppy, R., 2011. Debris-flood reconstruction in a pre-alpine catchment in Switzerland based on tree-ring records of coniferous and broadleaved trees. Geogr. Ann. A 93, 1–15.
Borga, M., Gaume, E., Creutin, J.D., Marchi, L., 2008. Surveying flash flood response: gauging the ungauged extremes. Hydrol. Process. 22 (18), 3883–3885.
Borga, M., Stoffel, M., Marchi, L., Marra, F., Jakob, M., 2014. Hydrogeomorphic response to extreme rainfall in headwater systems: flash floods and debris flows. J. Hydrol. 518 B, 194–205.
Breñosa, R., Castellarnau, J.M., 1884. Guía y descripción del Real Sitio de San Ildefonso. Sucesores de Rivadeneyra, Madrid.
Carling, P.A., 1986. The Noon Hill flash floods, July 17th 1983. Hydrological and geomorphological aspects of a major formative event in an upland landscape. Trans. Inst. Br. Geogr. 11, 105–118.
Cook, E.R., 1985. A time series analysis approach to tree-ring standardization. PhD Dissertation, University of Arizona, Tucson.
Corona, C., Lopez Saez, J., Stoffel, M., Bonnefoy, M., Richard, D., Astrade, L., Berger, F., 2012. How much of the real avalanche activity can be captured with tree rings? An evaluation of classic dendrogeomorphic approaches and comparison with historical archives. Cold Reg. Sci. Technol. 74–75, 31–42.
Corona, C., Lopez Saez, J., Stoffel, M., Rovéra, G., Edouard, J.L., Berger, F., 2013. Seven centuries of avalanche activity at Echalp (Queyras massif, southern French Alps) as inferred from tree rings. The Holocene 23, 292–304.
Corona, C., Lopez Saez, J., Stoffel, M., 2014. Defining optimal sample size, sampling design and thresholds for dendrogeomorphic landslide sampling. Quat. Geochronol. 22, 72–84.
Cortesi, N., Trigo, R., González-Hidalgo, J.C., Ramos, A.M., 2012. High resolution reconstruction of monthly precipitation of Iberian Peninsula using circulation weather types. Hydrol. Earth Syst. Sci. Discuss. 9, 6935–6977.
De Jong, C., Lawler, D., Essery, R., 2009. Perspective on climate impacts, snow seasonality and hydrological change in mountain environments. Hydrol. Process. 23, 955–961.
Díez Herrero, A., Laín Huerta, L., Martín-Duque, J.F., Vicente Rodado, F., 2008. A todo riesgo II. Convivir con los desastres geológicos cotidianos. Guión de la excursión científico-didáctica de la Semana de la Ciencia 2008, IGME, UCM e IE Universidad, Madrid-Segovia.
Dones, J., Garrido, M., 2001. Daños por temporales en el monte pinar de Valsaín. Datos históricos y problemas generados por el temporal de enero de 1996. III Congreso Forestal Español. 21–28/09/2001, Granada, Spain.
Foulds, S.A., Griffiths, H.M., Macklin, M.G., Brewer, P.A., 2014. Geomorphological records of extreme floods and their relationship to decadal-scale climate change. Geomorphology 216, 193–207.
Gestengabe, R.W., Werner, P.C., 2005. Katalog der Grosswetterlagen Europas (1881–2004) Nach Paul Hess Und Helmut Brezowsky. 6, Verbesserte und Ergänzte Auflage, PIK Report No. 100, Potsdam Institut Für Klimafolgenforschung, 153pp (in German).
Gottesfeld, A.S., 1996. British Columbia flood scars: maximum flood-stage indicator. Geomorphology 14, 319–325.
Gottesfeld, A.S., Gottesfeld, L.M.J., 1990. Flood-plain dynamics of a wandering river: Dendrochronology of the Maurice River, British Columbia, Canada. Geomorphology 3, 159–179.
Hupp, C.R., 1988. Plant ecological aspects of flood geomorphology and paleoflood history. In: Baker, V., Kochel, R., Patton, P. (Eds.), Flood Geomorphology. John Wiley & Sons, New York, pp. 335–356.
Ibsen, M.L., Brunsden, D., 1996. The nature, use and problems of historical archives for the temporal occurrence of landslides, with specific reference to the south coast of Britain, Ventnor, Isle of Wight. Geomorphology 15, 241–258.
Jakob, M., 2005. Debris flow hazard analysis. In: Jakob, M., Hungr, O. (Eds.), Debris flow hazards and related phenomena. Praxis Publishing, Chichester, UK, pp. 411–438.
Kingston, D.G., McGregor, G.R., Hannah, D.M., Lawler, D.M., 2007. Large-scale climatic controls on New England river flow. J. Hydrometeor. 8, 367–379.
Kogelnig-Mayer, B., Stoffel, M., Schneuwly-Bollschweiler, M., Hübl, J., Rudolf-Miklau, F., 2011. Possibilities and limitations of dendrogeomorphic time-series reconstructions on sites influenced by debris flows and frequent snow avalanche activity. Arct. Antarct. Alp. Res. 43 (3), 649–658.
Kundzewicz, Z.W., Stoffel, M., Kaczka, R., Wyzga, B., Niedzwiedz, T., Pinskwar, I., Ruiz-Villanueva, V., Lupikasza, E., Czajka, B., Ballesteros-Canovas, J.A., Malarzewski, L., Chorynski, A., 2014. Floods at the northern foothills of the Tatra Mountains – A Polish-Swiss research project. Acta Geophys. 62 (3), 620–641.
Lopez-Saez, J., Corona, C., Stoffel, M., Gotteland, A., Berger, F., Liebault, F., 2011. Debris-flow activity in abandoned channels of the Manival torrent reconstructed with LiDAR and tree-ring data. Nat. Hazard. Earth. Sys. 11, 1247–1257.
Marchi, L., Borga, M., Preciso, E., Gaume, E., 2010. Characterisation of selected extreme flash floods in Europe and implications for flood risk management. J. Hydrol. 394 (1–2), 118–133.
Mayer, B., Stoffel, M., Bollschweiler, M., Hübl, J., Rudolf-Miklau, F., 2010. Frequency and spread of debris floods on fans: a dendrogeomorphic case study from a dolomite catchment in the Austrian Alps. Geomorphology 118, 199–206.
Merz, B., Aerts, J., Arnberg-Nielsen, K., Baldi, M., Becker, A., Bichet, A., Blöschl, G., Bouwer, L.M., Brauer, A., Cioffi, F., Delgado, J.M., Gocht, M., Guzzetti, F., Harrigan, S., Hirschboeck, K., Kilsby, C., Kron, W., Kwon, H.H., Lall, U., Merz, R., Nissen, K., Salvatti, P., Swierczynski, T., Ulbrich, U., Viglione, A., Ward, P.J., Weiler, M., Wilhelm, B., Nied, M., 2014. Floods and climate: emerging perspectives for flood risk assessment and management. Nat. Hazards Earth Syst. Sci. Discuss. 2, 1559–1612.
Morales, C., Ortega, M.T., 2002. Las inundaciones en Castilla y Leòn. Eria 59, 305–332.
Parajka, J., Kohnová, S., Bálint, G., Barbuc, M., Borga, M., Claps, P., Cheval, S., Dumitrescu, A., Gaume, E., Hlavčová, K., Merz, R., Pfaundler, M., Stancalie, G., Szolgay, J., Blöschl, G., 2010. Seasonal characteristics of flood regimes across the Alpine–Carpathian range. J. Hydrol. 394 (1–2), 78–89.
Peel, M.C., Finlayson, B.L., McMahon, T.A., 2007. Updated world map of the Köppen-Geiger climate classification. Hydrol. Earth Syst. Sci. Discuss. 4 (2), 439–473.
Potenciano, A., 2004. Las inundaciones históricas en el centro-sur de la Península Ibérica. Condicionantes geomorfológicos y climáticos. PhD, Universidad Complutense, Madrid.
Ruiz-Villanueva, V., Diez-Herrero, A., Stoffel, M., Bollschweiler, M., Bodoque, J.M., Ballesteros, J.A., 2010. Dendrogeomorphic analysis of flash floods in a small ungauged mountain catchment (Central Spain). Geomorphology 118, 383–392.
Ruiz-Villanueva, V., Díez-Herrero, A., Bodoque, J.M., Ballesteros, J.A., Stoffel, M., 2013. Characterization of flash floods in small ungauged mountain basins of central Spain using an integrated approach. Catena 110, 32–43.
Salgueiro, A.R., Machado, M.J., Barriendos, M., Garcia-Pereire, H., Benito, G., 2013. Flood magnitudes in the Tagus River (Iberian Peninsula) and its stochastic relationship with daily North Atlantic Oscillation since mid-19th Century. J. Hydrol. 502, 191–201.
Schneuwly-Bollschweiler, M., Stoffel, M., 2012. Hydrometeorological triggers of periglacial debris flows in the Zermatt valley (Switzerland) since 1864. J. Geophys. Res. 117, F02033. http://dx.doi.org/10.1029/2011JF002262.
Schneuwly-Bollschweiler, M., Corona, C., Stoffel, M., 2013. How to improve dating quality and reduce noise in tree-ring based debris-flow reconstructions. Quat. Geochronol. 18, 110–118.
Schneuwly, D.M., Stoffel, M., Bollschweiler, M., 2009a. Formation and spread of callus tissue and tangential rows of resin ducts in *Larix decidua* and *Picea abies* following rockfall impacts. Tree Physiol. 29 (2), 281–289.
Schneuwly, D.M., Stoffel, M., Dorren, L.K.A., Berger, F., 2009b. Three-dimensional analysis of the anatomical growth response of European conifers to mechanical disturbance. Tree Physiol. 29 (10), 1247–1257.
Schraml, K., Kogelnig, B., Scheidl, C., Stoffel, M., Kaitna, R., 2013. Estimation of debris flood magnitudes based on dendrogeomorphic data and semi-empirical relationships. Geomorphology 201, 80–85.
Shroder, J.F., 1980. Dendrogeomorphology: review and new techniques of tree-ring dating. Prog. Phys. Geogr. 4, 161–188.
Sigafoos, R., 1964. Botanical Evidences of Floods and Flood-Plain Deposition. United States Government Printing Office.
Sigafoos, R., Hendricks, E.L., 1961. Botanical Evidence of the Modern History of Nisqually Glacier. United States Government printing office, Washington.
St. George, S., Nielsen, E., 2003. Paleofloods records for the Red River, Manitoba, Canada derived from anatomical tree-ring signatures. Holocene 13, 547–555.
Stoffel, M., 2008. Dating past geomorphic processes with tangential rows of traumatic resin ducts. Dendrochronologia 26 (1), 53–60.
Stoffel, M., Hitz, O.M., 2008. Snow avalanche and rockfall impacts leave different anatomical signatures in tree rings of *Larix decidua*. Tree Physiol. 28 (11), 1713–1720.
Stoffel, M., Corona, C., 2014. Dendroecological dating of geomorphic disturbance in trees. Tree-Ring Res. 70 (1), 3–20.
Stoffel, M., Wilford, D.J., 2012. Hydrogeomorphic processes and vegetation: disturbance, process histories, dependencies and interactions. Earth Surf. Proc. Land. 37, 9–22.
Stoffel, M., Liévre, I., Conus, D., Grichting, M., Raetzo, H., Gartner, H.W., Monbaron, M., 2005a. 400 years of debris flow activity and triggering weather conditions: Ritigraben, Valais, Switzerland. Arct. Antarct. Alp. Res. 37 (3), 387–395.
Stoffel, M., Schneuwly, D., Bollschweiler, M., Lièvre, I., Delaloye, R., Myint, M., Monbaron, M., 2005b. Analyzing rockfall activity (1600–2002) in a protection

forest a case study using dendrogeomorphology. Geomorphology 68 (3–4), 224–241.
Stoffel, M., Conus, D., Grichting, M.A., Lièvre, I., Maître, G., 2008. Unraveling the patterns of late Holocene debris-flow activity on a cone in the central Swiss Alps: chronology, environment and implications for the future. Glob. Planet. Change 60, 222–234.
Stoffel, M., Bollschweiler, M., Butler, D.R., Luckman, B.H., 2010. Tree rings and natural hazards: a state-of-the-art. Springer, Heidelberg, Berlin, New York.
Stoffel, M., Bollschweiler, M., Beniston, M., 2011. Rainfall characteristics for periglacial debris flows in the Swiss Alps: past incidences – potential future evolutions. Clim. Change 105, 263–280.
Stoffel, M., Butler, D.R., Corona, C., 2013. Mass movements and tree rings: a guide to dendrogeomorphic field sampling and dating. Geomorphology 200, 106–120.
Tomás, C., De Pablo, F., Rivas, L., 2004. Circulation weather types and cloud-to-ground flash density over the Iberian Peninsula. Int. J. Climatol. 24, 109–123.
Touchan, R., Meko, D.M., Ballesteros-Cánovas, J.A., Sánchez-Salguero, R., Camarero, J.J., Kerchouche, D., Muntán, E., Khabcheche, M., Blanco, J.A., Rodriguez-Morata, C., Garófano-Gómez, V., Martín, L.A., Alfaro-Sánchez, R., Garah, K., Hevia, A., Madrigal-González, M., Sánchez-Miranda, A., Shestakova, T.A., Tabakova, M., 2013. Dendrochronology course in Valsaín Forest, Segovia, Spain. Tree-Ring Res. 69 (2), 93–100.
Trigo, R.M., Pozo-Vázquez, D., Osborn, T.J., Castro-Díez, Y., Gámiz-Fortis, S., Esteban-Parra, M.J., 2004. North Atlantic oscillation influence on precipitation, river flow and water resources in the Iberian Peninsula. Int. J. Climatol. 24, 925–944.
Trigo, R.M., Varino, F., Ramos, A.M., Valente, M.A., Zêzere, J.L., Vaquero, J.M., Gouveia, C.M., Russo, A., 2014. The record precipitation and flood event in Iberia in December 1876: description and synoptic analysis. Front. Earth Sci. 2 (3), 1–15.